

# CHAPTER V

*Progress toward the In Vivo  
Visualization of Individual Bacterial  
Proteins after N-Terminal Labeling*

## **ABSTRACT**

In previous chapters, we have taken advantage of the orthogonality exhibited by NMT toward the bacterial proteome. This feature of NMT enabled in-lysate surface coupling of three different proteins that had been labeled by NMT, as summarized in Chapter IV. Here, we describe efforts toward applying NMT-mediated protein labeling to the selective functionalization of bacterial proteins of interest in order to visualize them in live cells and study their localization patterns.

Our initial attempts at such imaging experiments were complicated by the fact that thorough washing was not sufficient to remove unbound 12-ADA from cells; in fact, 12-ADA may be incorporated into the cell membrane by endogenous enzymes. Thus, we sought a different azide fatty acid that would be transferred by NMT to substrate proteins, but that could also be washed out of cells. We found that 7-azidoheptanoic acid fulfilled both of these criteria, as described in this chapter. We also selected two proteins for initial studies, PyrG and MreB, both of which are known to undergo spatiotemporal localization in bacterial cells. Cloning and expression were completed for both proteins, and an engineered MreB construct was found to be robustly labeled by NMT in live cells with both 7-azidoheptanoic acid and 12-ADA. These results will be useful in future applications of the NMT-mediated protein labeling system to detailed imaging studies of bacterial protein organization.

## **INTRODUCTION**

### ***Organization and Localization of Bacterial Proteins***

It has long been believed that bacteria do not exhibit sophisticated spatiotemporal orchestration of their proteins and other biomolecules. Biology textbooks have generally depicted mammalian cells in great detail, with complex organelles that migrate precisely in space and time, while describing prokaryotes in more simple terms. In a marked shift, recent research has shown that bacteria actually do organize and localize their proteins to a much greater degree than previously thought.<sup>1-3</sup> Powerful imaging techniques, such as stochastic optical reconstruction microscopy (STORM) and electron cryotomography (ECT), have enabled scientists to study bacteria at resolutions that are orders of magnitude higher than those offered by traditional light microscopy.<sup>2,4</sup> These developments and changes in the state of the field are summarized in the following selection from an essay written by Professor Bonnie Bassler, a leading microbiologist at Princeton University:

“Eukaryotes have long been known to possess sophisticated subcellular architecture in which DNA, RNA, and proteins are localized to the right place at the right time. Bacteria, in contrast, have until recently been thought to be unorganized bags of goop. Consequently, cell biology was generally restricted to eukaryotes. However, remarkable recent advances in imaging technologies... have made it so that we can now peer into bacterial cells as we traditionally peered into bigger eukaryotic cells. These technologies have revealed that bacteria are decidedly organized.” (*Adapted from Reference 5.*)

### ***NMT-Mediated Protein Labeling for Imaging Studies in Bacteria***

After developing the GFP/NMT model system described in Chapter II and confirming that NMT is selective toward engineered substrate proteins in bacteria, we recognized that NMT-mediated protein labeling could be a very useful tool for visualizing and studying individual bacterial proteins. By adding an NMT recognition sequence to a bacterial protein of interest, we postulated that we could selectively label the protein with 12-ADA and react it with a cyclooctyne dye for imaging. To test this hypothesis, we first attempted to utilize the original model system: Fyn-GFP and hNMT2 were co-expressed in bacteria in the presence of 12-ADA, and cells were treated with a cyclooctyne-lissamine-rhodamine dye. Initial results seemed promising, though the control experiment shown in Figure V-1 yielded an unexpected result: some cells appeared fluorescent even when no substrate protein was expressed.

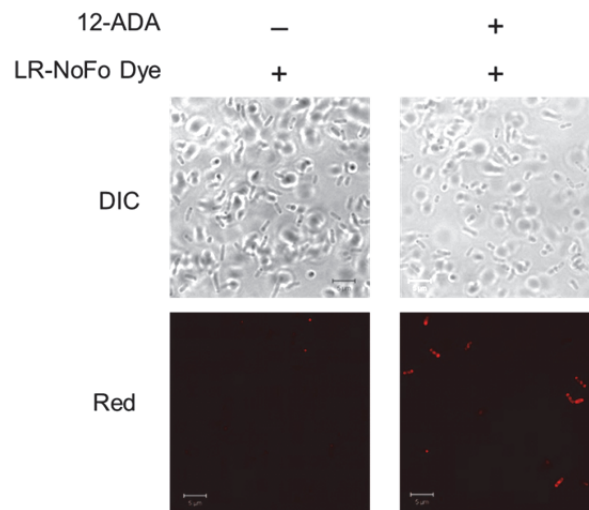


**Figure V-1.** Confocal microscope images of live cells expressing no NMT substrate protein, after reaction with lissamine-rhodamine non-fluorinated cyclooctyne dye (LR-NoFo). Cells that were not exposed to 12-ADA were dark (left panels), while prior exposure to 12-ADA yielded a fluorescence signal (right panels), despite the lack of a substrate protein for NMT to label with 12-ADA.

Based on the work described in Chapter II, we were confident that NMT was not labeling endogenous bacterial proteins. Thus, we concluded that 12-ADA, unlike the LR-NoFo dye, was not removed from cells by standard wash conditions that are compatible with live cells. In fact, 12-ADA may be transported into cells by bacterial enzymes responsible for the uptake of exogenous fatty acids; these fatty acids may then serve different functions within the cell, including structural roles in the cell membrane.<sup>6</sup> In any case, 12-ADA appeared to be interacting with bacterial cells in a manner that rendered it unsuitable for our proposed live-cell imaging studies.

In subsequent sections of this chapter, we describe our investigation of other azide fatty acids (FAs) to use in place of 12-ADA for imaging experiments. Specifically, we tested azide FAs with shorter chain lengths, searching for at least one that would be (a) bound and transferred by NMT to a substrate protein, and (b) washed out of cells in its free form without the use of harsh wash conditions. Using a combination of lysate and live-cell dye-labeling experiments, we identified a promising candidate, 7-azidoheptanoic acid. The azide FAs that we tested and the experimental outcomes are described below.

### ***PyrG and MreB***

In addition to finding a suitable azide FA for imaging experiments, we also undertook the task of engineering two bacterial proteins for labeling by NMT. The proteins we selected are PyrG and MreB, shown in Figure V-2.

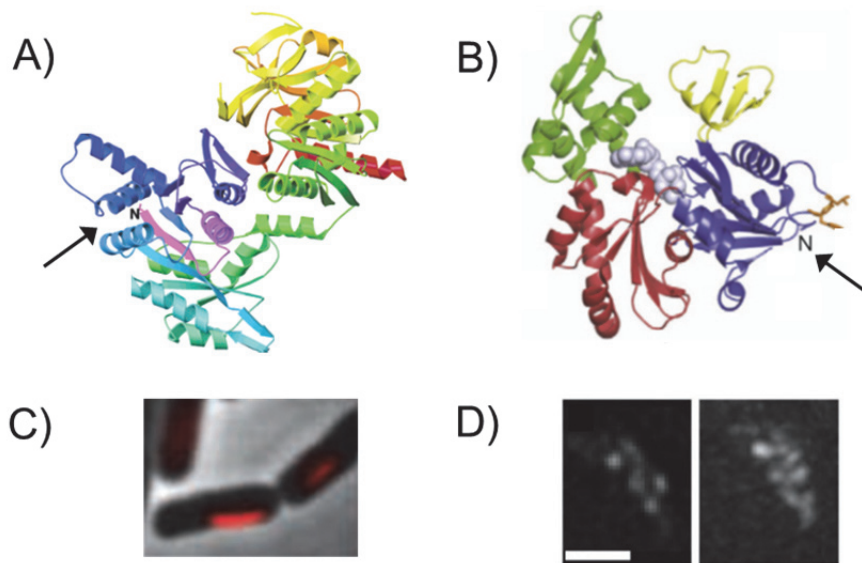


**Figure V-2.** Overview of the structures and localization patterns of PyrG and MreB. The black arrows point to the N-terminus on the crystal structures of PyrG (A) and MreB (B). In both proteins, the N-terminus appears to be surface-accessible. Confocal images of mCherry fluorescent protein fusions to PyrG (C) and MreB (D) in *E. coli* show that PyrG forms straight filamentous structures, while MreB adopts a helical pattern along the length of the cell. Adapted from References 7-10.

PyrG is a 60-kDa enzyme involved in converting UTP to CTP, and it also plays important structural roles in the cell; the interplay between its enzymatic and physical functions is currently under investigation.<sup>9</sup> PyrG is the *E. coli* homolog of a protein known as Ctp synthase (CtpS) in other bacterial species, such as *C. crescentus*.<sup>9</sup> As shown in Figure V-2C, an mCherry-PyrG fusion protein was shown to form long filamentous structures along the cell membrane; PyrG also self-assembles into filaments in its purified form.<sup>9</sup> We selected PyrG for further studies involving NMT labeling because it assembles into clear structures and also appears to perform interesting functions in the cell.

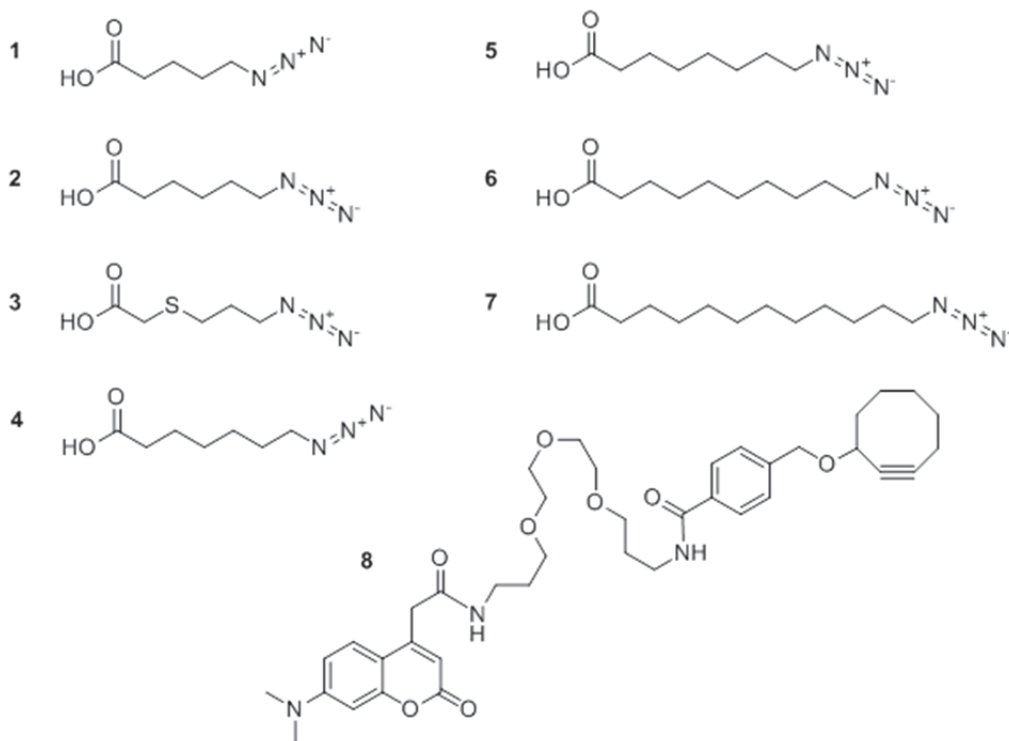
MreB is the primary bacterial homolog of actin.<sup>11</sup> Like PyrG, this 37-kDa protein has been expressed, purified, and structurally characterized. The crystal structure depicted in Figure V-2B is of the *Thermotoga maritima* form of MreB, which is 54% identical (70% related) to the *E. coli* form. In cells, MreB appears to assemble into filaments that in turn organize into a helical structure along the length of the cell (Figure V-2D). The length of the individual filaments is under continued investigation,<sup>12</sup> but they appear to play a role in maintaining the overall structure of the cell as well as contributing to cell motility.<sup>10</sup> We selected MreB for NMT-mediated protein labeling studies because, like PyrG, it forms interesting structures in the cell, and it is an early example of a bacterial protein whose localization patterns are actively regulated *in vivo*.

## **RESULTS AND DISCUSSION**

### ***Studies of Azide Fatty Acid Analogs: Dye-Labeling Lysate***

The structures of the azide FAs described in this chapter are shown in Chart V-1.

**Chart V-1.** Azide fatty acids (azide FAs) and cyclooctyne-coumarin dye utilized for *in vivo* labeling studies in bacteria. FA 7 is 12-ADA.



The azide FAs (**1-7**) were prepared by a former post-doctoral scholar in the Tirrell Group, Dr. Janek Szychowski, in a manner similar to that described in Chapter II for the synthesis of 12-ADA. The cyclooctyne-coumarin dye (**8**) utilized for the *in vivo* experiments described later in this chapter was prepared as previously described, also by Dr. Szychowski.<sup>13</sup> Cyclooctyne **8** is known to cross the cell membrane of mammalian cells and react selectively with azide-tagged biomolecules without harming cells. Its use in bacteria has not yet been reported, though we surmised that it would behave similarly in *E. coli* as in mammalian cells.

First, we investigated the extent to which each of the azide FAs was transferred by NMT to a substrate protein. For these experiments, we utilized the Fyn-GFP/hNMT2

co-expression system described in Chapter II. Protein expression, cell harvesting, and cell lysis were carried out as previously described; the only difference was that no fatty acid or one of the azide FAs in Chart V-1 was added to the expression flasks instead of 12-ADA when inducing protein expression. Lysates were treated with alkyne-TAMRA to enable detection of azide-labeled protein, as described in Chapters II and III, and analyzed by SDS-PAGE (Figure V-3).

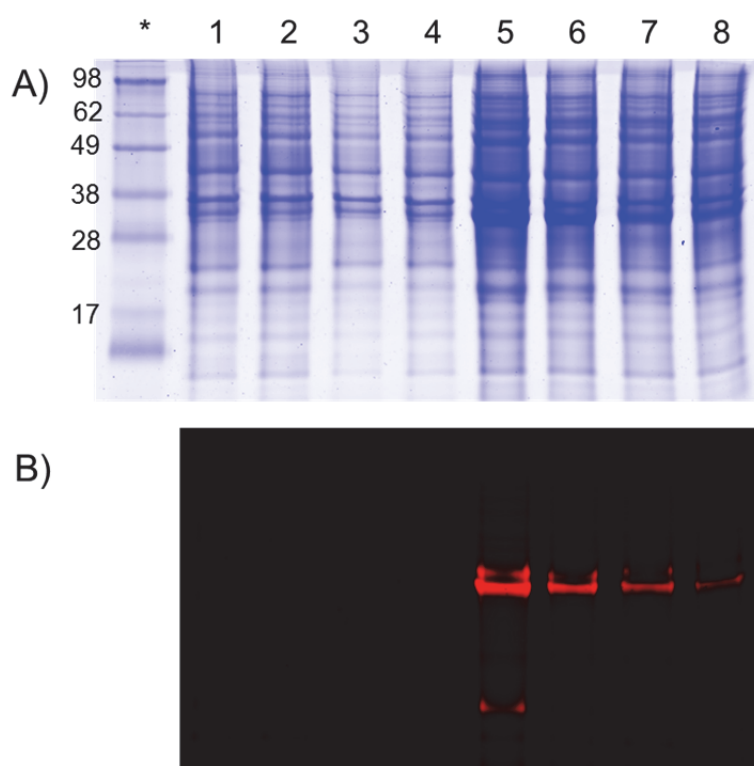


**Figure V-3.** SDS-PAGE analysis of lysate samples from Fyn-GFP/hNMT2 co-expression cultures exposed to different azide FAs. Samples were treated with alkyne-TAMRA for detection of azide-labeled Fyn-GFP. The gel was stained with Coomassie colloidal blue (A) and imaged for TAMRA signal (B). Fluorescent bands indicate successful and selective transfer of an azide FA onto Fyn-GFP. Lanes correspond to cultures exposed to the following azide FAs: 1: no fatty acid; 2: FA 1, 3: FA 2, 4: FA 3, 5: FA 4, 6: FA 5, 7: FA 6, 8: FA 7.

We were pleased to find that azide FA **4**, i.e., 7-azidoheptanoic acid, and FAs longer than **4** were appended by NMT to Fyn-GFP, as evidenced by the fluorescent bands in Figure V-3B (Lanes 5-8). The brighter appearance of the fluorescent band in the FA **4** lane (Lane 5) compared to the fluorescent bands for FAs **6** and **7** (Lanes 7-8) is simply an artifact of differences in protein loading across lanes, as confirmed by similar experiments culminating in SDS-PAGE analysis; when lanes were equally loaded with protein samples, we observed brighter TAMRA fluorescence for FAs **6** and **7**, as might be expected (data not shown). The sharp drop-off in signal for azide FAs shorter than **4** is in agreement with *in vitro* work carried out by the Gordon Lab with FAs possessing alkyl chains of varying lengths.<sup>14</sup>

One other notable feature of the gel image in Figure V-3B is the weak second band in the FA **4** lane (Lane 5). It is possible that FAs **4** and **5**, 7-azidoheptanoic acid and 8-azidooctanoic acid, respectively, may be utilized by lipoic acid ligase (also known as lipoate protein ligase) to label its substrate proteins; use of octanoic acid by this enzyme instead of lipoic acid has been documented when the concentration of lipoic acid is low or the concentration of octanoic acid is particularly high.<sup>15</sup> We found in separate experiments that titrating just 100  $\mu$ M free lipoic acid into the expression system eliminated the second band altogether (data not shown). Thus, if background labeling of lipoic acid ligase substrates with FA **4** does appear to interfere with visualizing a protein of interest during live-cell imaging, then addition of a small amount of lipoic acid should address the problem. However, given that the lower band in Lane 5 is significantly weaker than the Fyn-GFP band, this issue may not even arise in the context of microscopy experiments.

***Studies of Azide Fatty Acid Analogs: Dye-Labeling Live Cells***

Next, we examined how effectively each of the azide FAs **1-7** could be washed out of cells. In the first set of experiments described here, no substrate protein was expressed, yielding an experimental set-up similar to that in Figure V-1. Four hours after the addition of no fatty acid or one of the azide FAs **1-7** to the expression flask, cells were harvested, but were not lysed. Instead, samples were thoroughly washed, treated with cyclooctyne-coumarin **8**, washed again, and analyzed on a 96-well plate reader. Coumarin fluorescence as well as cell density were measured so that fluorescence measurements could be normalized. Both FA **1** and FA **4** produced a very low fluorescence signal (Figure V-4), indicating that those FAs were effectively washed out of cells prior to dye-labeling. Interesting, FAs **1** and **4** are both relatively short and possess an odd number of carbons.

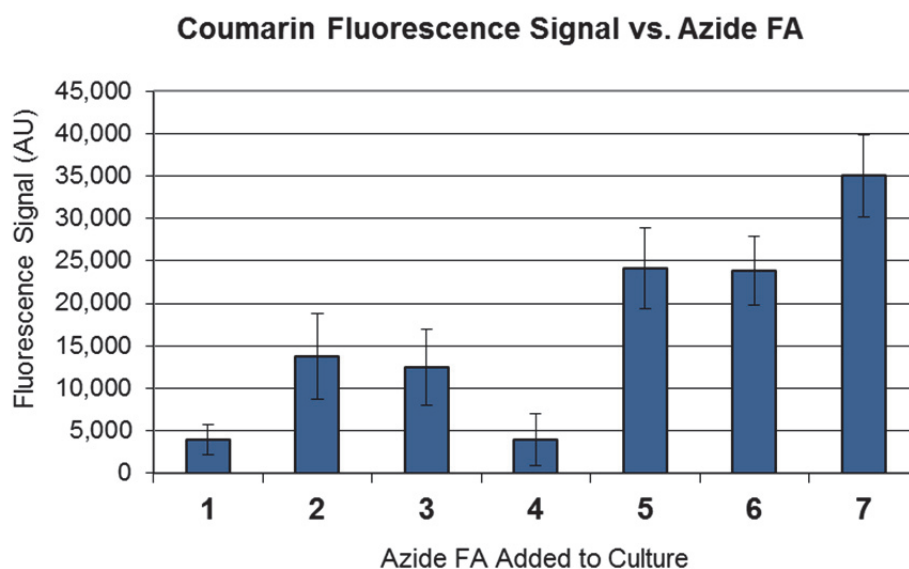


**Figure V-4.** Fluorescence signal of live *E. coli* cells after addition of an azide FA to the growth culture and subsequent dye-labeling with cyclooctyne-coumarin **8**. The azide FA added to each culture is

denoted as in Chart V-1. Each fluorescence value represents the average of a triplicate set of identical cultures,  $\pm$  standard deviation. Fluorescence values were normalized by cell density ( $OD_{600}$ ) and were background-corrected via subtraction of the fluorescence value of a control culture that was treated with **8** but not exposed to a FA. These experiments identified azide FA **4** as a promising candidate for *in vivo* labeling studies.

In a follow-up set of experiments, we again tested FAs **4** and **7** (7-azidoheptanoic acid and 12-ADA, respectively), now alongside additional controls. We grew cultures and dye-labeled cells as above, but we also prepared a sample that was exposed to neither a fatty acid nor cyclooctyne-coumarin **8**, and a sample that was exposed to myristic acid and **8**. These controls provided some insight into the potential interference of cellular autofluorescence (i.e., the sample not treated with **8**), the degree of nonspecific interaction between **8** and cellular components (i.e., the sample exposed to **8** but not to a fatty acid), and the degree of nonspecific interaction between **8** and an unreactive fatty acid (i.e., sample exposed to **8** and myristic acid). Furthermore, we grew parallel cultures in which no substrate protein was expressed or Fyn-GFP and hNMT2 were co-expressed.

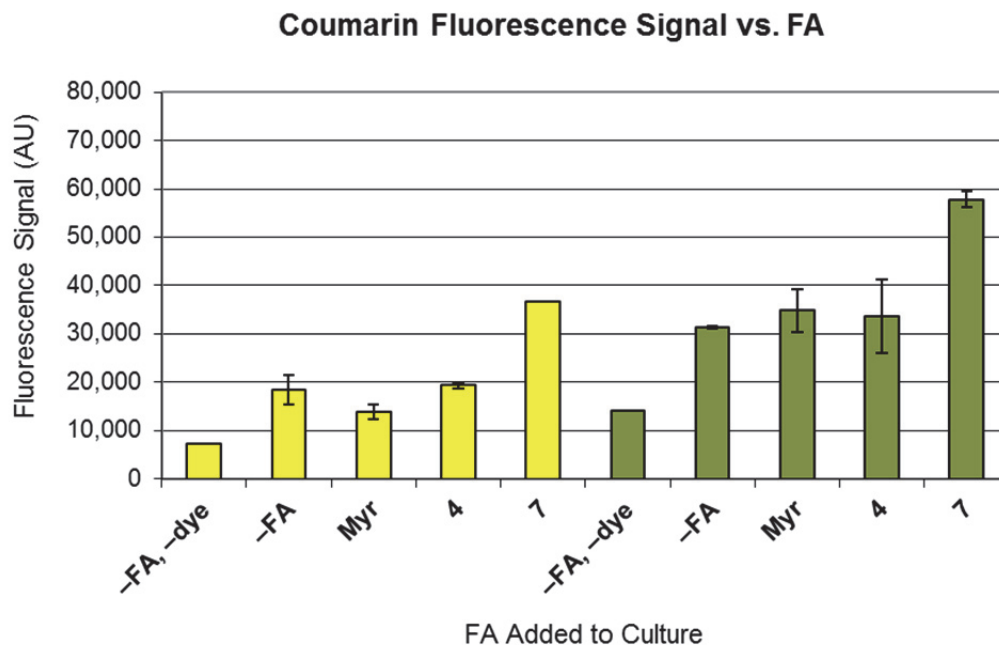


**Figure V-5.** Fluorescence signal of live *E. coli* cells after addition of no FA (“-FA”), myristic acid (“Myr”), or an azide FA (**4** or **7**), followed by dye-labeling with cyclooctyne-coumarin **8**. Cells exposed to neither a FA nor **8** (“-FA, -dye”) served as a control. Cells expressed no substrate protein (yellow bars) or co-expressed Fyn-GFP and hNMT2 (green bars). Each fluorescence value represents the average of a duplicate set of identical cultures,  $\pm$  standard deviation. All fluorescence signals were normalized by cell density ( $OD_{600}$ ).

The data, summarized in Figure V-5, provide some interesting results. We were pleased to find that the fluorescence of cultures to which **4** was added was similar to that of cultures exposed to no fatty acid or to myristic acid prior to dye-labeling with **8**. This similarity indicates that the fluorescence observed for cultures exposed to **4** is essentially background fluorescence due to some coumarin dye remaining in cells after washing, unrelated to the fatty acid alkyl chain or the azide moiety of **4**. The results also indicate that almost half the background signal in each set of samples is simply cellular

autofluorescence, as illustrated by the “-FA, -dye” samples. As expected, cultures exposed to **7** were considerably brighter than cultures exposed to **4** and the three controls. This result is in line with the observations associated with Figure V-1: azide FA **7** is not removed from cells by standard wash procedures and consequently reacts with cyclooctyne-coumarin **8**.

Surprisingly, the fluorescence signal for the Fyn-GFP/hNMT2 culture exposed to **7** was almost double that of the culture exposed to **4**, despite dye-labeling experiments in lysate (Figure V-3B) indicating that NMT transfers **4** to Fyn-GFP as well as it transfers **7**. It is possible that cyclooctyne-coumarin **8**, though membrane-permeable in mammalian cells, does not cross the bacterial cell membrane/cell wall to the same extent; in this scenario, most of the fluorescence in our live-cell experiments would arise from alkyne-reactive cell membrane components (i.e. azide FA **7**) rather than proteins inside the cell (i.e. Fyn-GFP labeled with **4** or **7**) reacting with **8**. Future work probing the behavior and membrane permeability of coumarin **8** in live bacteria should elucidate the cause of this discrepancy.

Finally, it may be worthwhile to confirm that FA **4** is not elongated or otherwise processed within the cell prior to binding by NMT. The methods described in Chapters II and III for whole-protein LC-MS studies would be readily applicable to this problem: Fyn-GFP co-expressed with NMT in the presence of FA **4** would be purified and subjected to LC-MS, in order to verify the appearance of a mass shift corresponding to the addition of one molecule of FA **4**. It seemed unlikely that enzymatic elongation is occurring, given the difference in data sets obtained for FAs **4** and **7** in live-cell dye-

labeling experiments. Thus, we moved forward as planned with experiments involving engineered substrate proteins.

For experiments with engineered PyrG and MreB constructs, described in the next section, we proceeded with FA **4**, 7-azidoheptanoic acid, which fulfills both criteria established earlier for an azide FA to be suitable for imaging studies: FA **4** is transferred to substrate proteins by NMT, and free FA **4** is removed from live cells upon completion of a standard wash protocol.

### ***Preparation and Evaluation of yARF-PyrG and yARF-MreB Constructs***

As noted earlier, the bacterial proteins PyrG and MreB were selected for NMT-mediated protein labeling studies. Both proteins were engineered to display the yARF NMT recognition sequence (MGLFASK) described in Chapters II and III. Rather than using a recombinant plasmid as the PCR template, as we had done for all previous cloning projects, we used genomic DNA isolated from *E. coli* cells as the template for PCR amplification. The final yARF-PyrG and yARF-MreB constructs were transformed into *E. coli* BL21(DE3) competent cells already harboring the hNMT1 plasmid. Co-expression cultures were grown in LB medium as described in Chapters II and III, with the addition of no fatty acid, **4**, or **7** when protein expression was induced. Samples were collected at regular time points (30, 60, 90, and 120 min) to monitor cell density, protein expression, and extent of protein labeling for each culture. Growth curves are presented first, in Figure V-6.

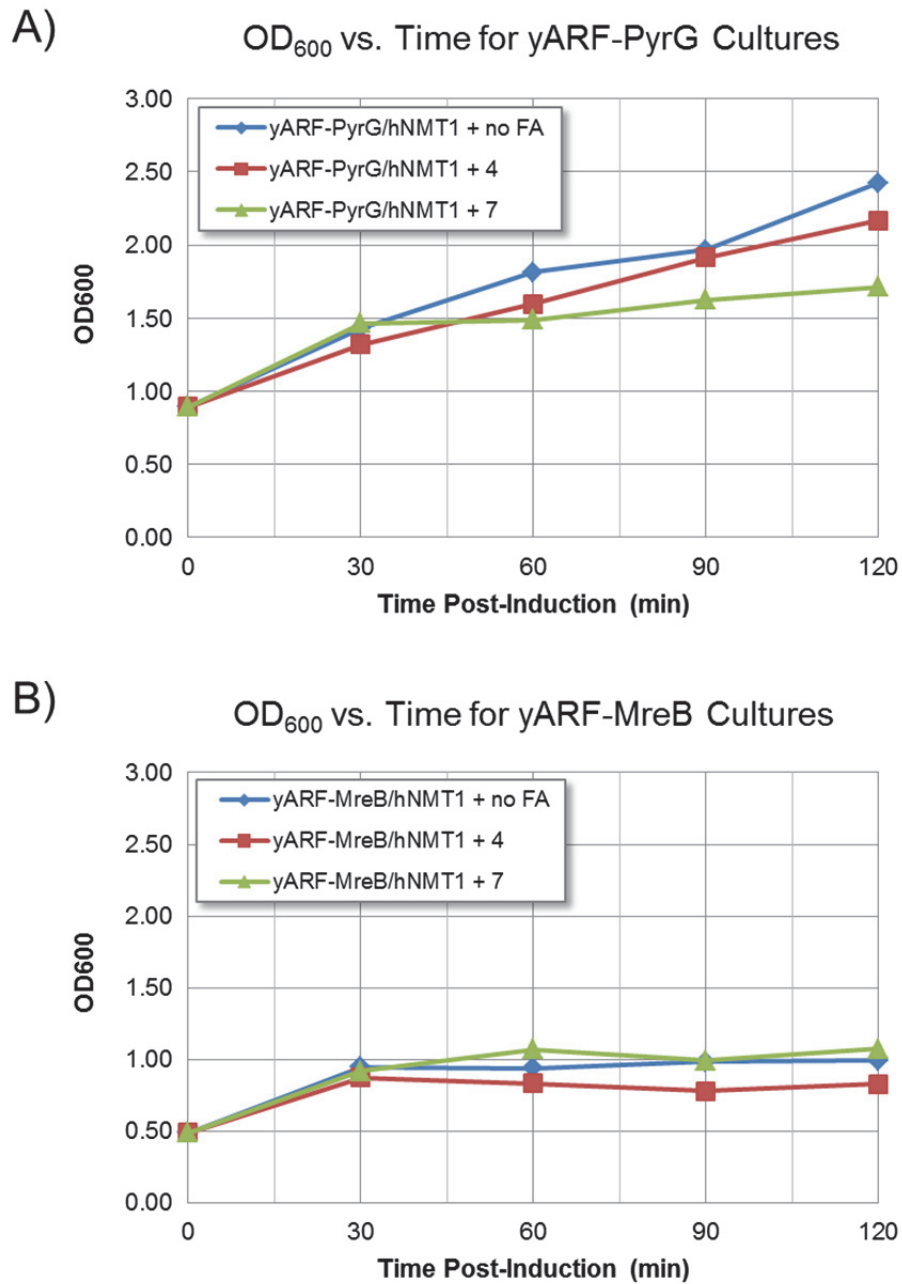


**Figure V-6.** Growth rates for co-expression cultures of yARF-PyrG/hNMT1 (A) and yARF-MreB/hNMT1 (B). Cell density (OD<sub>600</sub>) was measured at 30-min intervals and plotted as a function of time. Addition of an azide FA (4 or 7) does not appear to impact cell growth for either protein. Expression of yARF-MreB has a larger effect on cell growth than expression of yARF-PyrG.

In contrast with our earlier work involving GFP, CaN, and CaM, the experiments in this chapter involve engineered versions of proteins that are endogenous to bacteria and that perform important functions for proper cell functioning. Thus, we were curious how the expression of yARF-PyrG or yARF-MreB and addition of **4** or **7** would affect cell growth, as measured by cell density ( $OD_{600}$ ). For both the yARF-PyrG/hNMT1 and yARF-MreB/hNMT1 cultures, addition of an azide FA appeared to have little or no impact on growth rates, an encouraging sign with regard to utilizing NMT-mediated protein labeling to study bacterial proteins. Expression of yARF-PyrG did not appear to impact cellular health as measured by cell density, which increased normally with time. However, expression of yARF-MreB did have a negative effect on growth, evidenced by a plateau in cell density after induction. For future work, it will be worthwhile to place each construct under the control of native promoters in order to achieve endogenous levels of protein expression, as well as to limit expression to the appropriate times and places in the cell. It will also be important to examine any changes to protein structure and function resulting from addition of an NMT recognition sequence and 12-ADA.

At each time point, cells were also collected and lysed in order to determine the level of protein expression and the extent of labeling by NMT. Lysate samples were treated with alkyne-TAMRA, precipitated, resuspended, and analyzed by SDS-PAGE, as described in Chapters II and III. Examination of the results for yARF-PyrG (Figure V-7) indicate that the protein is expressed rapidly and robustly, though almost no NMT labeling is observed. It is possible that the yARF-PyrG protein N-terminus is inaccessible to NMT in the protein's folded state; it could be that the assembly of PyrG monomers into filaments blocks access to the N-terminus of individual protein

monomers; or in either of these scenarios, it is possible that the N-terminus is indeed labeled by NMT but is inaccessible for reaction with alkyne-TAMRA. One or more of these factors, or others, could contribute to the lack of yARF-PyrG labeling by NMT, despite high expression levels.

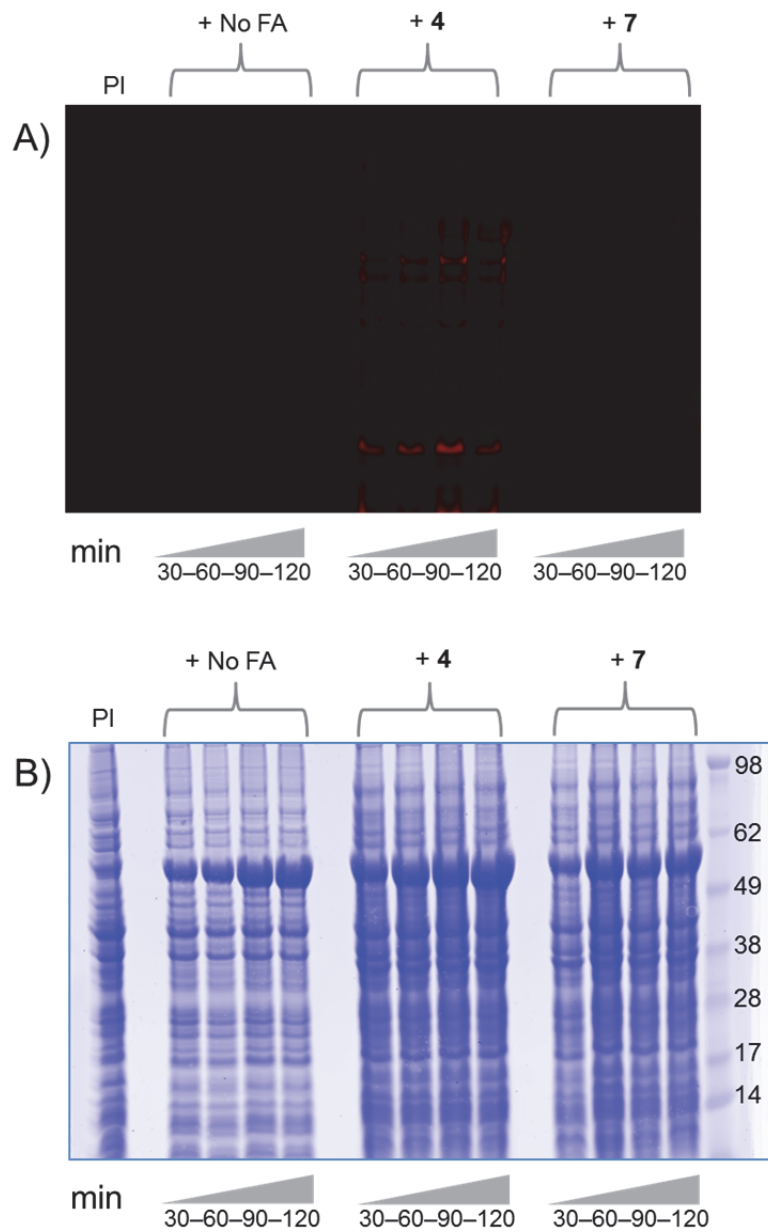


**Figure V-7.** SDS-PAGE analysis of lysate samples from yARF-PyrG/hNMT1 co-expression cultures to which no FA, azide FA 4, or azide FA 7 was added. Bacterial culture samples were collected at 30, 60, 90, and 120 min, and resultant lysates were treated with alkyne-TAMRA for detection of azide-labeled yARF-PyrG. The gel was imaged for TAMRA signal (A) and stained with Coomassie colloidal blue (B). The lack of fluorescent bands indicates poor labeling of yARF-PyrG by NMT, though the strong Coomassie-stained bands near 62 kDa indicate successful expression.

Identical experiments were carried out with samples from yARF-MreB/hNMT1 co-expressions. Again, lysate samples were treated with alkyne-TAMRA, precipitated, resuspended, and analyzed by SDS-PAGE. The results shown in Figure V-8 indicate that yARF-MreB expresses well and is labeled by NMT with either FA **4** or **7**, a promising finding with regard to using **4** for future imaging studies. Furthermore, high levels of protein expression and labeling were observed for yARF-MreB within just 30 min. We anticipate that even shorter expression times could be used, thus providing a more accurate snapshot of yARF-MreB localization at a given point in time or in response to a particular stimulus.

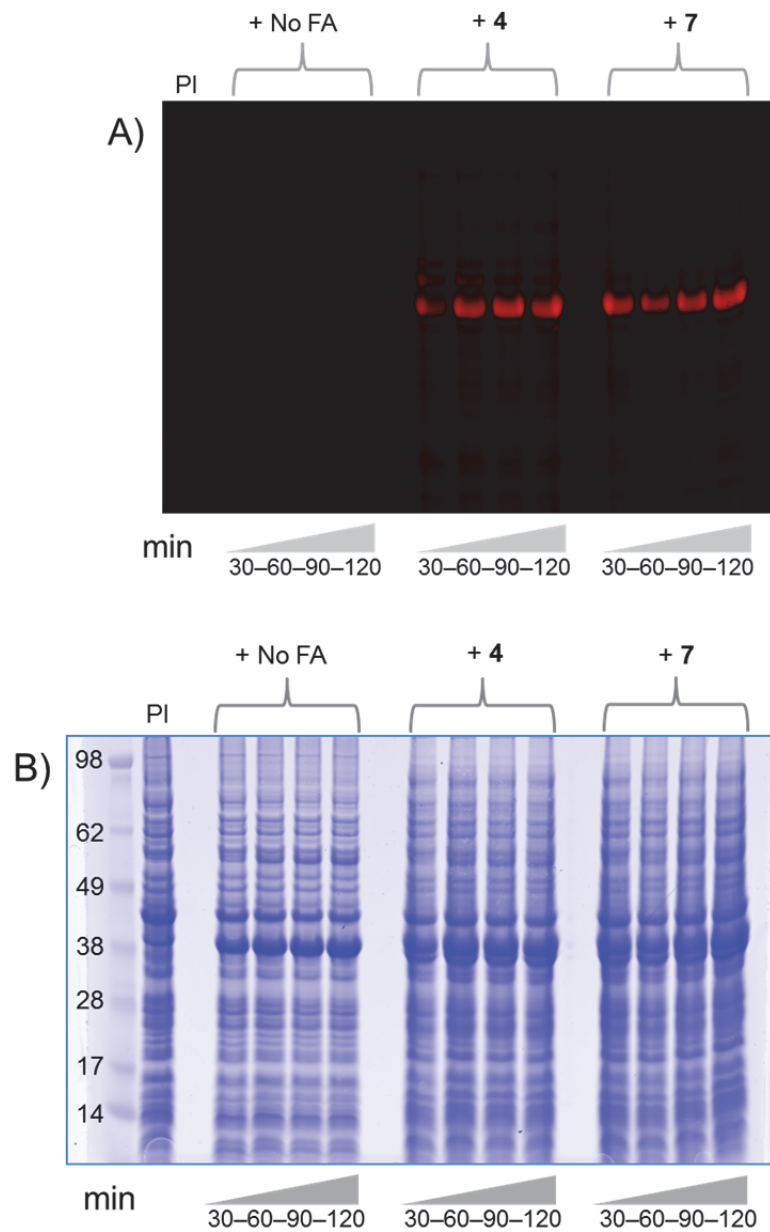


**Figure V-8.** SDS-PAGE analysis of lysate samples from yARF-MreB/hNMT1 co-expression cultures to which no FA, azide FA 4, or azide FA 7 was added. Bacterial culture samples were collected at 30, 60, 90, and 120 min, and resultant lysates were treated with alkyne-TAMRA for detection of azide-labeled yARF-MreB. The gel was imaged for TAMRA signal (A) and stained with Coomassie colloidal blue (B). The strong Coomassie-stained bands near 38 kDa and the corresponding TAMRA bands indicate rapid expression of yARF-MreB and robust labeling by NMT.

## CONCLUSION

We have developed and evaluated nearly all of the necessary components to apply NMT-mediated protein labeling to the selective *in vivo* visualization of specific bacterial proteins. As with the GFP-based model system described in Chapter II, a reactive fatty acid, NMT, and a substrate protein are required. We evaluated a family of azide fatty acids with varying chain lengths and identified 7-azidoheptanoic acid as a promising candidate for imaging studies: our experiments demonstrate that this azide fatty acid is transferred to substrate proteins by NMT, like 12-ADA, and can be washed out of cells, unlike 12-ADA. We also prepared two novel non-natural substrates for NMT labeling, yARF-PyrG and yARF-MreB, derived from proteins that exhibit interesting localization patterns in cells. Cloning and expression of both constructs was successful, and yARF-MreB was shown to be labeled efficiently by NMT with 7-azidoheptanoic acid.

The final steps in this project include placement of yARF-MreB under the control of endogenous promoters, investigation of the impact of protein engineering and labeling on yARF-MreB, and ultimately, completion of live-cell imaging experiments. Options for protein visualization include the treatment of cells with a cyclooctyne fluorophore followed by confocal microscopy, or possibly the use of ECT with an appropriate probe. In addition, the cloning and protein labeling methods summarized herein could be applied to other proteins of interest in bacteria. The progress described here is a promising start towards employing NMT in detailed studies of the complex and fascinating internal environment of bacterial cells.

## **EXPERIMENTAL SECTION**

### ***Materials***

**Synthesis of azide fatty acids.** The starting materials (bromo-, iodo-, or chloro-acids) were purchased from Aldrich. Silica gel 60 was purchased from EMD Chemicals. Sodium azide and all solvents were purchased from VWR.

**Lysate studies with azide fatty acids.** The BL21(DE3)/Fyn-GFP/hNMT2 bacterial co-expression system was described in Chapter II. A control cell strain lacking pQE80\_Fyn-GFP was also used. LB medium was composed of 10 g tryptone (casein hydrolysate), 5 g yeast extract, and 10 g NaCl per liter. All media was autoclaved before use. Kanamycin (Kan) was used at a working concentration of 35  $\mu\text{g}/\text{mL}$ , and ampicillin (Amp) was used at a working concentration of 200  $\mu\text{g}/\text{mL}$ . Myristic acid was purchased from Fluka. All optical density (OD) values were measured at 600 nm on a Cary UV-Vis spectrophotometer. Lysate samples were treated with the reagents and according to the protocols of the Click-IT Tetramethylrhodamine (TAMRA) Protein Analysis Detection Kit from Invitrogen. Lysis Buffer was 1% SDS, 50 mM Tris-HCl, pH 8.0, as recommended by Invitrogen. After reaction with alkyne-TAMRA and precipitation, protein samples were run on Invitrogen NuPAGE Novex 4–12% Bis-Tris pre-cast gels and imaged on a GE Typhoon laser scanner. Gels were stained with Coomassie colloidal blue from Invitrogen.

**Live-cell dye-labeling studies with azide fatty acids.** Materials for expression cultures are as indicated above for “Lysate studies with azide fatty acids,” though cells were not lysed after harvesting. Instead, cells were dye-labeled with cyclooctyne-coumarin, prepared by Dr. Janek Szychowski as previously reported,<sup>13</sup> and washed with phosphate-buffered saline (PBS). Fluorescence measurements were collected on a Tecan 96-well plate reader.

**Cloning.** All oligonucleotide primers were ordered from IDT. Polymerase chain reaction (PCR) experiments were carried out in a BioRad DNA Engine Peltier Thermal Cycler using PfuTurbo DNA Polymerase (Stratagene/Agilent). Genomic DNA, isolated

from *E. coli* BL21 (DE3) cells with the Qiagen DNEasy kit, served as the template DNA for PCR reactions. All restriction enzymes, restriction enzyme buffers, bovine serum albumin (BSA), and ligase were purchased from New England BioLabs (NEB). NEB DNA Ladders (100 bp and 1 kbp “Quick-Load”) were used as markers for all DNA agarose gels, which were visualized with the addition of Plus One ethidium bromide solution from Amersham Biosciences on a UVP UV Transilluminator. Zymo Agarose-Dissolving Buffer (ADB) and Zymo Spin II columns, with their associated buffers, were used to purify DNA out of agarose gels. All plasmid DNA acquisition from cells was completed using the Qiagen Spin Miniprep Kit and columns. All sequencing requests were fulfilled by Laragen.

**Time-course growth and expression studies.** BL21(DE3)/yARF-PyrG/hNMT1 and BL21(DE3)/yARF-MreB/hNMT1 cell strains were prepared by transforming each final construct in pQE80 into BL21(DE3) competent cells already harboring the hNMT1 plasmid. The plasmid encoding hNMT1 and methionine-aminopeptidase (Met-AP) was a gift from the laboratory of Professor Richard Kahn at Emory University (Atlanta, GA).<sup>16</sup> Otherwise, all materials are identical to those listed above for “Lysate studies with azide fatty acids.”

## ***Methods***

**Synthesis of azide fatty acids.** Azide fatty acids were prepared by Dr. Janek Szychowski with methods similar to those described in Chapter II for the synthesis of 12-azidododecanoic acid (12-ADA). The starting material for each compound was the bromo-, iodo-, or chloro-acid. After reaction with sodium azide and a work-up procedure, each compound was isolated by rotary evaporation and characterized by ESI-MS and <sup>1</sup>H NMR.

**Lysate studies with azide fatty acids.** The BL21(DE3)/Fyn-GFP/hNMT2 bacterial co-expression system, described in Chapter II, was utilized for studies with the different azide FAs. (Control cultures lacking pQE80\_ Fyn-GFP were also grown.) In summary, overnight cultures were diluted into fresh LB, and expression cultures were

grown in an incubator-shaker (37°C, 250 rpm). Protein expression was induced with IPTG (1 mM, from 1 M stock in water) when the OD<sub>600</sub> value was between 0.8 and 1.1. (In control cultures lacking pQE80\_Fyn-GFP, no protein expression was induced.) Either no fatty acid or one of the azide fatty acids in Chart V-1 (500 μM, from 500 mM stock in DMSO) was also added at the time of induction. After 4 hr of protein expression, cells were harvested via centrifugation and the final OD<sub>600</sub> value was measured. Cell pellets were lysed according to the following formula: 50 μL Lysis Buffer per mL culture per OD<sub>600</sub> unit. Crude lysates were centrifuged once more, and the supernatant (clarified lysate) was reacted with alkyne-TAMRA according to the protocols supplied by Invitrogen, as described in Chapter II. Samples were precipitated following the methanol-chloroform precipitation protocol described in the same kit instructions, and they were analyzed by SDS-PAGE. To detect TAMRA signal on the Typhoon, the 532 nm laser served as the excitation source (filter set: 580 BP 30). Gels were stained with Coomassie colloidal blue, then imaged again, with the 633 nm laser now serving as the excitation source (no filter).

**Live-cell dye-labeling studies with azide fatty acids.** Cultures were grown identically as indicated above for “Lysate studies with azide fatty acids,” except that cells were not lysed after harvesting. Instead, cells were washed with PBS 3 times to remove excess azide FA, dye-labeled with 50 μM cyclooctyne-coumarin for 30 min at 37°C, and washed again to remove excess dye. Absorption and fluorescence measurements were collected on a plate reader. To measure the cells per unit volume, OD<sub>600</sub> was measured on the plate reader. To measure cyclooctyne-coumarin fluorescence, samples were excited at 380 nm (bandwidth: 5 nm) and signal was read at 475 nm (bandwidth: 5 nm). Fluorescence values were divided by OD<sub>600</sub> values for normalization.

**Cloning.** Genomic DNA isolated from *E. coli* BL21(DE3) cells served as the template DNA for preparation of both yARF-PyrG and yARF-MreB. Primers were designed to encode the yARF recognition sequence (MGLFASK, from ATG GGT CTG TTC GCG TCT AAA) at the 5' end of the gene and a 6xHis tag at the 3' end of the gene, as well as appropriate restriction sites. The yARF-PyrG and yARF-MreB PCR products

were digested with EcoRI and HindIII and ligated into pQE80 digested with the same enzymes. (Constructs were also prepared in pET-15b, though they were not utilized for further protein expression studies; similar PCR products were prepared, digested with NcoI and XhoI, and ligated into pET-15b that had been digested with the same enzymes.) All four constructs (pQE80\_yARF-PyrG, pQE80\_yARF-MreB, pET-15b\_yARF-PyrG, and pET-15b\_yARF-MreB) were transformed into DH-10b competent cells and plated. Colonies were selected for inoculation of cultures from which DNA was isolated and submitted for sequencing. Each final construct was transformed into competent cells already harboring an NMT plasmid for co-expression experiments.

**Time-course growth and expression studies.** Co-expression of yARF-PyrG or yARF-MreB with hNMT1 was performed in a manner identical to that described in Chapter II and summarized above in the “Lysate studies with azide fatty acids” section. When inducing protein expression with IPTG, no fatty acid, FA 4 (7-azidoheptanoic acid), or FA 7 (12-ADA) was also added to the expression flask (500  $\mu$ M, from 500 mM stock in DMSO). Samples were collected after 30 min, 60 min, 90 min, and 120 min of protein expression. At each time point, cells were harvested via centrifugation (10 min x 10,000 g at 4°C). To prepare growth curves, the OD<sub>600</sub> of each time-point sample was also measured on a UV-Vis spectrophotometer. Cell pellets were lysed according to the following formula: 50  $\mu$ L Lysis Buffer per mL culture per OD<sub>600</sub> unit. Crude lysates were centrifuged once more, and the supernatant (clarified lysate) was reacted with alkyne-TAMRA according to the protocols supplied by Invitrogen, as described in Chapter II. Samples were precipitated following the methanol-chloroform precipitation protocol described in the same kit instructions, and they were analyzed by SDS-PAGE. To detect TAMRA signal on the Typhoon, the 532 nm laser served as the excitation source (filter set: 580 BP 30). Gels were stained with Coomassie colloidal blue, then imaged again, with the 633 nm laser now serving as the excitation source (no filter).

## REFERENCES

1. Gitai, Z. The new bacterial cell biology: moving parts and subcellular architecture. *Cell* **120**, 577–86 (2005).
2. Jensen, G. J. & Briegel, A. How electron cryotomography is opening a new window onto prokaryotic ultrastructure. *Curr. Opin. Struct. Biol.* **17**, 260–7 (2007).
3. Shapiro, L., McAdams, H. H. & Losick, R. Why and how bacteria localize proteins. *Science* **326**, 1225–8 (2009).
4. Gitai, Z. New fluorescence microscopy methods for microbiology: sharper, faster, and quantitative. *Curr. Opin. Microbiol.* **12**, 341–6 (2009).
5. Bassler, B. L. Small cells—big future. *Mol. Biol. Cell* **21**, 3786–7 (2010).
6. Dirusso, C. C. & Black, P. N. Bacterial long chain fatty acid transport: gateway to a fatty acid-responsive signaling system. *J. Biol. Chem.* **279**, 49563–6 (2004).
7. Endrizzi, J. A., Kim, H., Anderson, P. M. & Baldwin, E. P. Crystal structure of Escherichia coli cytidine triphosphate synthetase, a nucleotide-regulated glutamine amidotransferase/ATP-dependent amidoligase fusion protein and homologue of anticancer and antiparasitic drug targets. *Biochemistry* **43**, 6447–63 (2004).
8. Van den Ent, F., Amos, L. A. & Löwe, J. Prokaryotic origin of the actin cytoskeleton. *Nature* **413**, 39–44 (2001).
9. Ingerson-Mahar, M., Briegel, A., Werner, J. N., Jensen, G. J. & Gitai, Z. The metabolic enzyme CTP synthase forms cytoskeletal filaments. *Nat. Cell Biol.* **12**, 739–46 (2010).
10. Gitai, Z., Dye, N. & Shapiro, L. An actin-like gene can determine cell polarity in bacteria. *Proc. Natl. Acad. Sci. U. S. A.* **101**, 8643–8 (2004).
11. Shaeviz, J. W. & Gitai, Z. The structure and function of bacterial actin homologs. *Cold Spring Harb. Perspect. Biol.* a000364 (2010).  
doi:10.1101/cshperspect.a000364
12. Swulius, M. T. *et al.* Long helical filaments are not seen encircling cells in electron cryotomograms of rod-shaped bacteria. *Biochem. Biophys. Res. Commun.* **407**, 650–5 (2011).

13. Beatty, K. E. *et al.* Live-cell imaging of cellular proteins by a strain-promoted azide-alkyne cycloaddition. *ChemBioChem* **11**, 2092–5 (2010).
14. Kishore, N. S. *et al.* Comparison of the acyl chain specificities of human myristoyl-CoA synthetase and human myristoyl-CoA: protein N-myristoyltransferase. *J. Biol. Chem.* **268**, 4889–902 (1993).
15. Perham, R. N. Swinging arms and swinging domains in multifunctional enzymes: catalytic machines for multistep reactions. *Annu. Rev. Biochem.* **69**, 961–1004 (2000).
16. Van Valkenburgh, H. A. & Kahn, R. A. Coexpression of proteins with methionine aminopeptidase and/or N-myristoyltransferase in *Escherichia coli* to increase acylation and homogeneity of protein preparations. *Methods Enzymol.* **344**, 186–93 (2002).